S8-05
98717
20 P.

MODELING XV-15 TILT-ROTOR AIRCRAFT DYNAMICS BY FREQUENCY AND TIME-DOMAIN IDENTIFICATION TECHNIQUES

by

Mark B.Tischler
Aeroflightdynamics Directorate
US Army Aviation Research and Technology Activity
Ames Research Center
Moffett Field, California 94035-1099, USA

Juergen Kaletka
Research Scientist
Deutsche Forschungs- und Versuchsanstalt
fuer Luft- und Raumfahrt e.V. (DFVLR)
Institut fuer Flugmechanik
D-3300 Braunschweig-Flughafen, Federal Republic of Germany

SUMMARY

Models of the open-loop hover dynamics of the XV-15 Tilt-Rotor Aircraft are extracted from flight data using two approaches: frequency-domain and time-domain identification. Both approaches are reviewed and the identification results are presented and compared in detail. The extracted models compare favorably, with the differences associated mostly with the inherent weighting of each technique. Step responses are used to show that the predictive capability of the models from both techniques is excellent. Based on the results of this study, the relative strengths and weaknesses of the frequency and time-domain techniques are summarized, and a proposal for a coordinated parameter identification approach is presented.

NOMENCLATURE

p,q,r	roll rate, pitch rate, and yaw rate, respectively, deg/sec
u,v,w	longitudinal, lateral, and vertical velocities, respectively, m/sec
γ^2_{xy}	coherence function between variable x and y
$\delta_a, \delta_e, \delta_r$	aileron surface deflection (deg), elevator surface deflection (deg), and rudder surface deflection (deg), respectively
δ_c	power lever deflection, %
ζ	damping ratio
τ	time delay
ϕ, θ, ψ	roll, pitch, and yaw angles, respectively, rad (deg)
ω	undamped natural frequency, rad/sec
1/T	inverse time constant, rad/sec

1. INTRODUCTION

Dynamics identification methodologies generally fall into two categories: frequency-domain and time-domain. The choice of techniques to be used is usually based on the analyst's personal familiarity with the methods and on the specific application. Each approach has inherent strengths and weaknesses. Frequency-domain identification uses spectral methods to determine frequency responses between selected input and output pairs. Then, least-squares fitting techniques are used in the frequency-domain to obtain closed-form analytical transfer-function models of linear input-to-output processes. Time-domain identification first requires the selection of a state-space model structure, which may be linear or nonlinear. Model parameters are identified by least-squares fitting of the response time-histories or by maximum likelihood methods. Transfer functions for linear models and frequency responses can then be obtained from the identified state-space formulation.

The US Army has been developing frequency-domain identification techniques in support of handling qualities, flight, and simulation experiments. Extensive flight experiments have been conducted on the

XV-15 Tilt-Rotor Aircraft (Fig. 1). References 1 and 2 present the identified open-loop frequency responses, transfer functions, and model verification results. Frequency-domain identification tests have also been recently conducted on the Bell-214-ST single (teetering) rotor, and CH-47 tandem-rotor aircraft (Refs. 3 and 4). In the Federal Republic of Germany, the DFVLR has had extensive experience with maximum-likelihood, time-domain identification techniques. Linear and nonlinear model-identification methods have been developed. Much of the DFVLR experience with helicopter identification has been associated with the highly coupled BO-105 hingeless-rotor helicopter (Refs. 5 and 6).

As part of an ongoing US/FRG Memorandum of Understanding (MOU) on helicopter flight control, an extensive joint study is being conducted to analyze the XV-15 data-base for the (open-loop) hover flight condition using both time- and frequency-domain techniques. The primary objectives of this study are to: (1) gain a better appreciation for the relative strengths and weaknesses of each technique; and (2) develop improved methods of identification for rotorcraft.

This paper reviews the dynamics identification techniques which have been developed in the US and the Federal Republic of Germany. The results of applying these techniques to the XV-15 data base are presented and compared, and sources of differences in the extracted models are discussed. Finally, conclusions concerning the appropriate applications for each technique and proposals for unified identification methods using both approaches are presented.

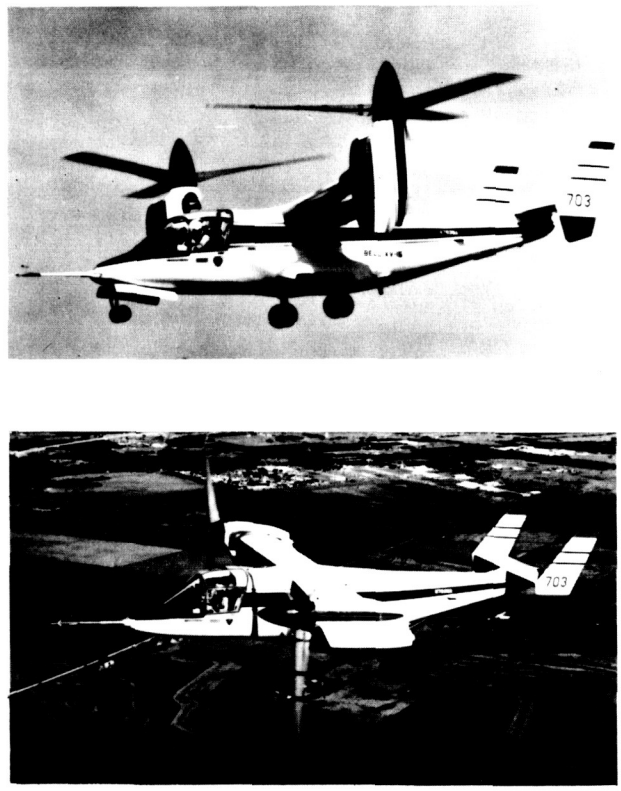

Fig. 1. The XV-15 Tilt-Rotor Aircraft. a) Hover configuration; b) cruise configuration.

2. OVERVIEW OF FREQUENCY-DOMAIN AND TIME-DOMAIN IDENTIFICATION TECHNIQUES

A. Frequency-Domain Identification Method

The frequency-domain identification approach developed by the US Army is depicted in Fig. 2. Spectral methods based on the Chirp z-transform are used to extract high-resolution frequency responses between selected input and output pairs. The identification results are presented in Bode-plot format: magnitude and phase of the output to the input versus frequency. These identification results are nonparametric because no model structure has been assumed. As such, they can be very useful for flight-control system design and handling-qualities compliance testing; for example, currently proposed handling-qualities criteria for the LHX (Ref. 7) are based on frequency-domain parameters which can be read directly from these graphical results. Frequency responses obtained from real-time and nonreal-time simulations can be compared directly with the flight data to expose limitations and discrepancies in the simulator models (Ref. 1). The fact that this comparison can be made initially without an a priori assumption of model structure or order is especially important for verifying mathematical models of new aircraft configurations. When the model structure and parameter values are required, they may be obtained by fitting the tabulated frequency-responses with analytical transfer-function models to extract modal characteristics. Examples of this application are the testing of handling-quality specifications given in

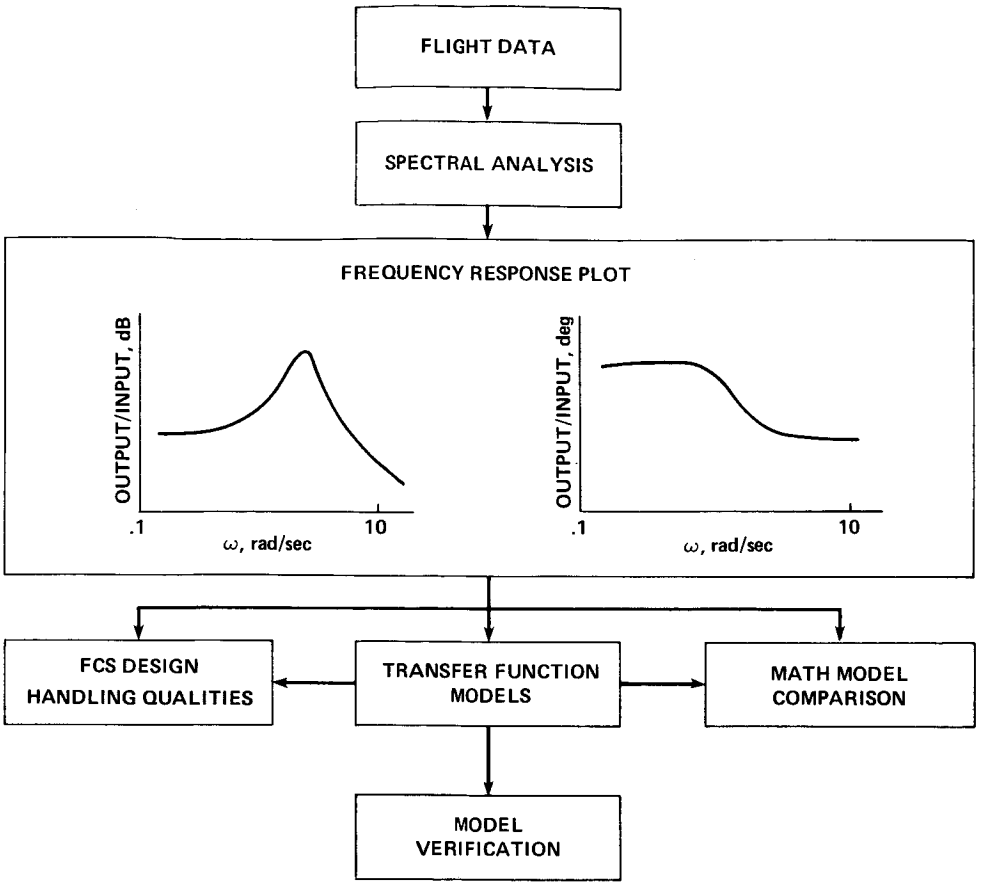

Fig. 2. Frequency-domain identification method.

lower-order equivalent system terms, and the examination of transfer function-based control system designs. Since this fitting procedure is completed after the frequency response is extracted, the order of the transfer function can be carefully selected to avoid an overparameterized model. Multi-input/multi-output frequency-response methods are suitable for extracting a transfer matrix which includes the important coupling effects. Finally, the extracted models are driven with the flight-test control inputs to verify the time-domain response characteristics.

The semilog frequency format of the Bode-plot presentation and subsequent transfer-function fit makes the identified transfer-function and state-space models most accurate at mid and high frequency (initial time history transients). The low-frequency and steady-state response prediction of the extracted models is generally not as good as in time-domain identification approaches.

B. Time-Domain Identification Method

The general approach used in time-domain identification is shown in Fig. 3. Time-based identification techniques are initially applied to the data to check their internal compatibility. Data inconsistencies resulting from calibration errors, drifts, or instrumentation failures are detected by comparing redundant measurements from independent sensors, such as rate and attitude gyros, or altitude change and vertical acceleration (Ref. 6). This approach, which can be used on-line, helps to ensure that only consistent data are generated for the further evaluation and system identification.

For this next step, the aircraft dynamics are modeled by a set of differential equations describing the external forces and moments in terms of accelerations and state and control variables. The coefficients in these equations are the stability-derivatives. In some cases, a priori values for these derivatives can be obtained from analytical calculations, wind-tunnel data, or from start-up identification techniques such as a least-squares method. The responses of the model and aircraft resulting from the flight-test control inputs are then compared. The response differences are minimized by the identification algorithm which iteratively adjusts the model parameters. In this sense, aircraft system identification implies the extraction of physically defined aerodynamic and flight mechanics parameters from flight-test data. Usually, it is an off-line procedure since some skill and iteration are needed to develop an appropriate model formulation. Model formulation involves consideration of model structure, selection of significant parameters, and inclusion of important nonlinearities. Time-domain techniques yield a multi-input/multi-output model that is appropriate for application in stability and control analysis, simulation, and control system design. The identified parameters are also useful for comparison and correction of analytically or wind-tunnel derived stability-derivatives (Ref. 8).

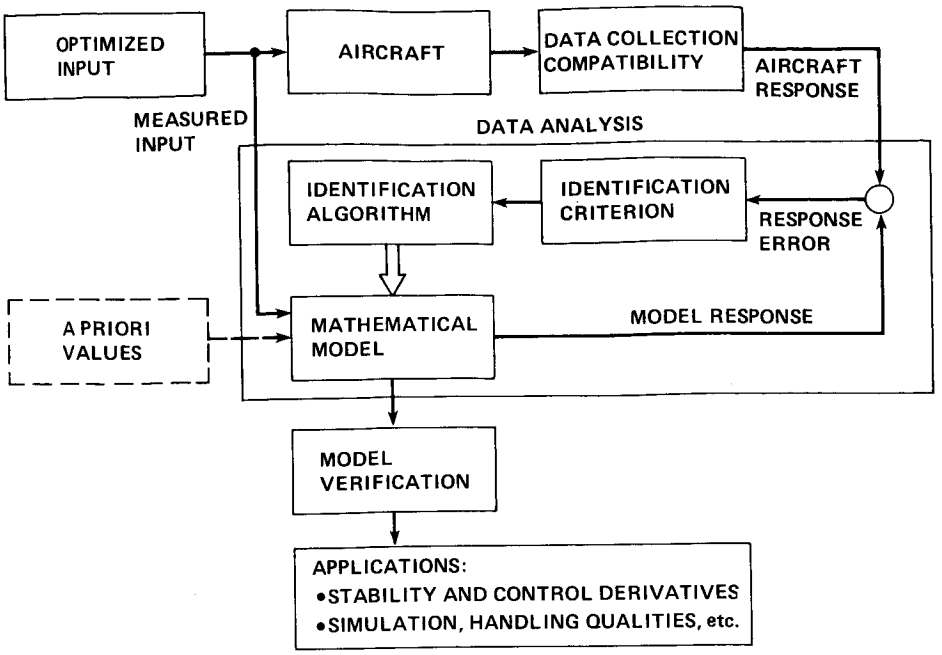

Fig. 3. Time-domain identification method.

A key feature of the time-domain identification technique is that the extracted models are based on the curve fitting of the original measured (time-domain) flight-test data. Errors which may occur in the transformation of the data from the time- to the frequency-domain are thus avoided. The identified models can then be easily presented in the frequency-domain as Bode plots or, if the identified model is linear, also as parametric transfer-functions.

3. IDENTIFICATION OF XV-15 OPEN-LOOP DYNAMICS IN HOVERING FLIGHT

This section reviews the XV-15 flight-test data base for parameter identification and presents and compares the results of (linear) frequency and time-domain identification methods for the open-loop hover flight condition. For illustrative purposes, the roll response identification is discussed in detail.

A. Flight-Test Data Base

The complete data base for dynamics identification includes four flight conditions from hover to cruise. The present study concentrated exclusively on the identification of the open-loop hover dynamics because:

The dynamics for this flight condition are coupled and very unstable which makes this case the most difficult to analyze.

Nonlinear effects are the most significant in the hover flight condition, which allows a good demonstration of the nonlinear identification techniques developed by the DFVLR.

Focusing on the rotor-borne flight condition maximizes the carry-over of the present experience to future rotorcraft identification studies to be carried out under the MOU.

The pitch and roll axis instabilities for the hover flight condition are characterized by a time-to-double amplitude of about 3 sec. Therefore, long-period inputs needed to identify the low-frequency vehicle dynamics are not practical for the open-loop hovering vehicle. Extraction of the open-loop vehicle dynamics from closed-loop testing is possible subject to an important condition: the total surface deflection, which is comprised of inputs from the pilot and the stability and control augmentation system (SCAS), must contain a significant component which is uncorrelated with the response of the vehicle (Ref. 9). Then, the required low-frequency inputs can be conducted on the closed-loop (stable) vehicle.

Flight-Test Inputs. Two types of inputs were executed in the identification flight tests. "Frequency-sweep" inputs were used for model extraction, and step inputs were used for model verification.

Two typical concatenated lateral stick frequency-sweeps completed during the hover flight tests of the XV-15 are shown in Fig. 4a. These tests used pilot-generated rather than computer-generated inputs. The sweep is initiated with two low-frequency input cycles corresponding to the lower bound of the frequency range of primary interest (0.2-6.0 rad/sec). These cycles ensure good excitation of the low-frequency vehicle dynamics. After the initial two low-frequency cycles, the lateral stick is oscillated at progressively higher frequencies for an additional 50 sec. By the end of the 90 sec duration test, the stick is being driven at fairly high frequencies (4 Hz shown in Fig. 4). The input amplitudes are fairly

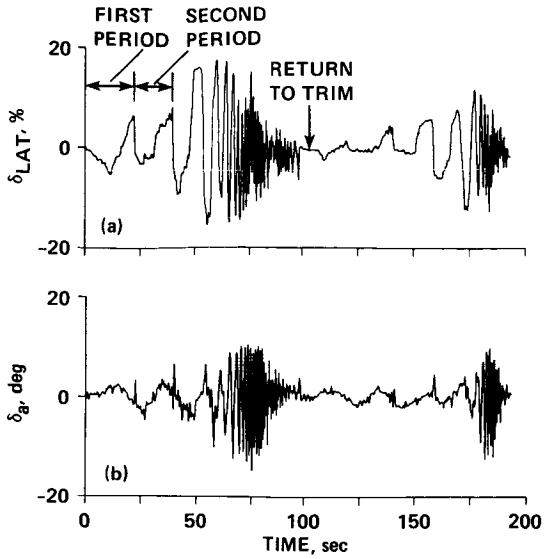

Fig. 4. Two lateral stick frequency-sweeps (δ_{LAT}) in hover. a) Lateral stick inputs; b) aileron surface deflections.

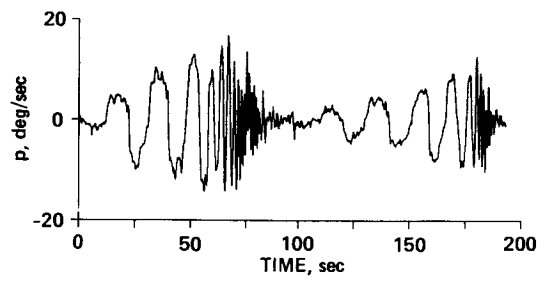

Fig. 5. Roll-rate response (p) during lateral frequency-sweeps.

small at low frequency where vehicle motions are considerable, with larger inputs at mid frequency, and smaller inputs again at very high frequency. The associated aileron surface deflection (total input to the aircraft‡) shown in Fig. 4b reflects a significant component from the pilot input (note that δ_a and δ_{LAT} are defined with opposing sign conventions). The resulting roll-rate amplitudes of 10-20 deg/sec as shown in Fig. 5 are typical for frequency-sweep tests. The frequency-sweep is especially well suited for frequency-domain identification because it is a periodic input form that excites the vehicle in all of its dominant modes of motion within the frequency range of interest. This input also has some advantages for time-domain identification. Vehicle excitation is restricted to be within the frequency-range of model applicability which is especially important for meaningful state-space parameter results (Ref. 4). Also, the monotonic increase in frequency allows the time-domain identification to be frequency-weighted which compensates for the inherent low-frequency weighting of this method.

Step inputs are commonly used in the flight test community to expose dominant vehicle characteristics, so they represent a good test of the identified model's predictive capability. Step inputs were executed in both the open- and closed-loop condition. Open-loop verification ensures that the identified models reflect the dynamics of the open-loop vehicle and not those of the inverse feedback element (Ref. 9). Step inputs with the flight-control system engaged are also useful since the steadier initial conditions allow fine differences between the model and the flight responses to be exposed.

B. Frequency-Domain Identification

The most important step in the frequency-domain identification procedure is the extraction of accurate, high-resolution frequency responses between the various input and output pairs. A key metric for assessing the quality of the frequency-response identification is the coherence function (γ^2_{xy}). This frequency-dependent function indicates that fraction of the output response which is linearly related to the excitation signal. The random error associated with the frequency-response identification is dependent on the value of the coherence function at each frequency, and on the number of (independent) time history segments ("windows," N_d):

‡Although the aileron, elevator, and rudder surfaces are not effective in hover, they continue to be actuated in addition to the primary effectors which are the rotor collective and swashplate controls. It was found to be most expedient to refer all the transfer functions to these surface deflections, since neglecting the small servo lags, these are related to the sum of the pilot and SCAS inputs through a mixing ratio which is constant across the entire flight envelope.

$$\varepsilon = \frac{[1 - \gamma_{xy}^2]^{1/2}}{|\gamma_{xy}|\sqrt{2N_d}} \quad (*) \tag{1}$$

The length of the window (secs) determines the amount of low-frequency power and the associated low-frequency coherence which can be achieved. Low variance in the spectral identification therefore requires high coherence and multiple concatenated time-history records. Initial analyses of the XV-15 data base used all available repeat runs (three were used in the original analysis of Ref. 1), without concern of the individual coherence quality of each run. Subsequent time-domain analyses by the DFVLR and frequency-domain analyses by the US Army indicated that some of the frequency-sweep runs were unsuitable for identification, and should be removed from the concatenation procedure. In the case of the lateral axis frequency-sweep, one of the three runs was found to be unsuitable because of low coherence. The frequency-response obtained with the remaining two (good) runs has substantially improved spectral quality. This frequency response and the associated coherence function are shown in Figs. 6 and 7. Good identification is achieved over the frequency range 0.2-9.0 rad/sec.

The magnitude response peak is due to the dominant roll modes which are in the frequency-range of 0.5-1 rad/sec; the associated phase rise indicates that the modes are unstable. At the higher frequencies (1.0-10 rad/sec), the magnitude and phase plots follow a K/s characteristic. The value of the constant (K) is the roll response sensitivity (L_{δ_a}). The relatively flat phase response at high frequency indicates a very small value of effective time delay. Finally, the drop in coherence function near the magnitude peak suggests the existence of nonlinearities for large vehicle motions.

(1) Lateral/Directional Transfer-Function Models

The selection of the order and structure of the transfer-function models is predominantly based on three important factors (Ref. 4):

(a) The models must be appropriate to the frequency-range of concern (0.2-6.0 rad/sec in the present study).

(b) The models must provide a reasonable fit of the input-to-output frequency response within the frequency range associated with good coherence.

(c) The selected models should be based on a theoretical analysis of the effective physical order of the system. Therefore, the appropriate transfer-function models are a function of flight condition and flight-control system status (i.e., SCAS-on or SCAS-off).

For the open-loop XV-15 in the hovering flight condition, the yaw (and heave) responses are essentially decoupled and first order in nature. Therefore, an appropriate model for yaw-rate response to pedal inputs is:

$$\frac{r}{\delta_r}(s) = \frac{N_{\delta_r} e^{-\tau_\psi s}}{(s + 1/T_y)} \tag{2}$$

The on-axis roll (and pitch) responses are dominated by the hovering cubic, and as seen in Fig. 6 have one excess pole at high frequency:

$$\frac{p}{\delta_a}(s) = \frac{L_{\delta_a} s(1/T_{\phi_1})(1/T_{\phi_2}) e^{-\tau_\phi s}}{(1/T_y)(1/T_r)[\zeta_r,\omega_r]} \quad (+) \tag{3}$$

The dominant source of coupling in the open-loop configuration is the yaw response to lateral stick inputs. This coupling arises from the rotor torque differential which accompanies the differential collective inputs used for roll control. Frequency-response identification of the coupled response (Ref. 1) indicates an appropriate transfer-function model of:

$$\frac{r}{\delta_a}(s) = \frac{N_{\delta_a}(1/T_\psi)[\zeta_\psi,\omega_\psi] e^{-\tau_{\psi_2} s}}{(1/T_y)(1/T_r)[\zeta_r,\omega_r]} \tag{4}$$

The denominator parameters of the lateral/directional transfer-function models (Eqns. 2-4) represent natural dynamics modes of the vehicle. Therefore, the common modes must have the same values for all three responses. Maintaining this relationship is essential for achieving unique and physically meaningful transfer-function models. While it is possible to fit all three responses simultaneously to maintain the commonality of denominator parameters, this approach is not the best. A better strategy is to identify individual parameters from the <u>on-axis</u> frequency-response in which they have the dominant effect.

---

*Window overlapping further reduces the random error below that shown in Eqn. (1) (Ref. 9).

+Shorthand notation: $[\zeta, \omega]$ implies $s^2 + 2\zeta\omega s + \omega^2$, ζ = damping ratio, ω = undamped natural frequency (rad/sec); and $(1/T)$ implies $s + (1/T)$, rad/sec.

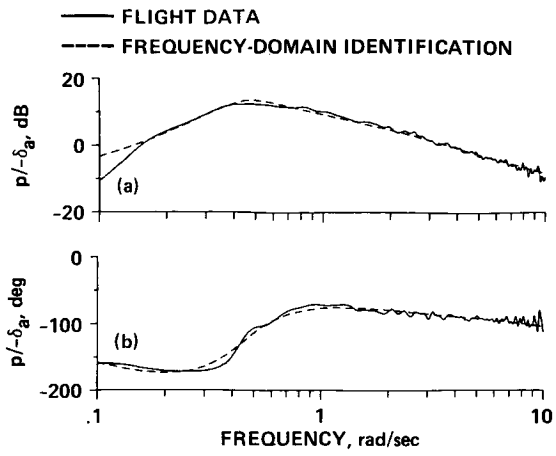

Fig. 6. Frequency-domain identification of roll-rate response to aileron ($p/-\delta_a$). a) Magnitude; b) phase.

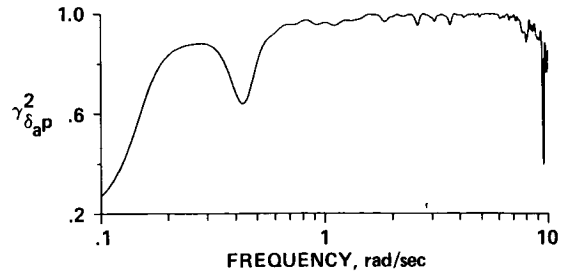

Fig. 7. Coherence function for roll-rate response identification ($\gamma^2_{\delta_a p}$).

Then these parameters are fixed in the identification of the off-axis transfer-functions. So, for example, the following yaw response transfer-function is obtained from the pedal sweeps:

$$\frac{r}{\delta_r}(s) = \frac{0.619\ e^{-0.0210s}}{(s + 0.102)} \tag{5}$$

This result shows that the yaw response of the tilt-rotor configuration is very lightly damped, as compared to a standard helicopter with a tail rotor. The small effective time delay indicates that lags caused by unmodeled high-frequency dynamics are negligible.

The next step is to identify the roll-rate transfer function (p/δ_a). Since the yaw mode has been identified in Eqn. 5, this parameter is fixed in the roll-response transfer function (Eqn. 3). Then the remaining parameters are varied to obtain the best least-squares fit of the roll rate frequency-response (Fig. 6):

$$\frac{p}{\delta_a}(s) = \frac{-3.71s(-0.107)(0.412)e^{-0.0313s}}{(0.102)(1.23)[-0.418,\ 0.447]} \tag{6}$$

The fitting range is from 0.2-9.0 rad/sec, in which the coherence function ($\gamma^2_{\delta_a p}$) indicates good spectral accuracy. As expected from the phase response characteristics (Fig. 6b), the open-loop roll-response dynamics are dominated by an unstable roll mode with the frequency of about 0.4 rad/sec. The associated time-to-double amplitude is 3.5 sec. The pole-zero pair $(1/T_{\phi_1})/(1/T_y)$ is at very low frequency and nearly cancels out. This reveals that yaw coupling does not noticeably affect the roll-response characteristics. Therefore, a lower-order roll response model which contains only the hovering (lateral) cubic roots $(1/T_r)[\zeta_r,\omega_r]$ and entirely ignores yaw coupling is an appropriate approximation for this vehicle. This assumption is common for hovering aircraft. The low-frequency numerator factor $(1/T_{\phi_1})$ associated with lateral translation damping, is marginally unstable (time-to-double amplitude = 7.5 sec) indicating a very low value of the velocity damping derivative (Y_v). Finally, the effective time delay for the roll response (τ_ϕ) is small, suggesting that, as in the yaw response (Eqn. 5), the unmodeled high-frequency lags are not significant.

With the lateral/directional denominator factors (dominant vehicle modes) identified using the on-axis frequency-responses, the numerator factors of the off-axis response (r/δ_a) can now be extracted. The denominator factors of Eqn. 4 are fixed and the least-squares fit gives:

$$\frac{r}{\delta_a}(s) = \frac{0.344(-0.345)[0.868,\ 0.487]e^{-0.00900s}}{(0.102)(1.23)[-0.418,\ 0.447]} \tag{7}$$

In the frequency range $\omega > 1.2$ rad/sec, the yaw response to aileron inputs is dominated entirely by the coupling derivative, N_{δ_a}. At low frequencies, the dynamics are affected by the unstable hovering cubic.

As shown in Figs. 6a and 6b, the transfer-function model of Eqn. 6 is a good representation of the identified roll response in the range of satisfactory coherence (0.2-9.0 rad/sec). Although the present transfer-function model (Eqn. 6) is not significantly different from that obtained previously (Ref. 1) using all of the available sweep runs (including the poor quality runs), the match between the model and flight data is significantly improved.

Close examination of Fig. 6 shows that the match between the model and flight data is much better in magnitude than in phase. This is because of the relative weighting selected for the identification (1 DB magnitude error: 7° phase error) which is common for lower-order equivalent system matching (Ref. 10). On the basis of the steep phase response of the flight data at the dominant mode (ω = 0.5 rad/sec) as compared to the transfer-function model, a lower (less negative) damping ratio is indicated. This inconsistency between the magnitude and phase responses indicates nonlinear behavior in the dominant modes of roll motion. As mentioned previously, this is also reflected by the drop in coherence in the same frequency range. Significant side-by-side nonlinear rotor interactions are known to exist for large lateral-velocity transients, as were encountered during the low-frequency inputs.

The lateral/directional transfer-function model results of this section are summarized in Table 1.

(2) Longitudinal Transfer-function Models

In hovering vehicles, pitch and roll dynamics are analogous. The pitch response is dominated by a longitudinal hovering cubic analogous to the lateral hovering cubic, and a first-order heave response is analogous to the first-order yaw response. Power lever (vertical control) and longitudinal stick inputs do not induce significant inter-axis coupling in the XV-15 configuration.

Spectral analysis of the individual pitch-sweeps showed that only one of the three runs had satisfactory coherence for use in identification. (The original analysis of Ref. 1 used all three runs.) Transfer-function models are extracted from the identified frequency responses using the same approach discussed above for the lateral/directional dynamics. The heave response is determined first from collective sweeps, and then the pitch response is determined with the identified heave mode ($1/T_h$) fixed. The resulting transfer functions for pitch rate and vertical acceleration responses are summarized in Table 1. As in the roll case, the pitch response is dominated by a hovering (longitudinal) cubic, comprised of a low-frequency unstable oscillation, [ζ_p, ω_p], and a stable aperiodic mode ($1/T_p$). Also, the pitch transfer-function model fits the identified frequency response much better in magnitude than in phase. Based on phase response considerations alone, the unstable damping ratio would, as before, be much lower (less negative). The discrepancy between the magnitude and phase fit is again due to nonlinearities associated with the large velocity perturbations encountered during the low-frequency inputs.

C. Time-Domain Identification

Maximum likelihood (ML) technique is generally accepted as one of the most suitable time-based methods for aircraft parameter identification. The main advantages of the ML estimation are:

(1) It yields asymptotically unbiased and consistent estimates for linear systems.

TABLE 1 Comparison of Transfer-Function Models for Hover

Frequency-Domain Identification	Time-Domain Identification
$\frac{r}{\delta_r}(s) = \frac{0.619\ e^{-0.0210s}}{(0.102)}$	$\frac{r}{\delta_r}(s) = \frac{0.732\ e^{-0.0320s}}{(0.0987)}$
$\frac{p}{\delta_a}(s) = \frac{-3.71s(-0.107)(0.412)e^{-0.0313s}}{(0.102)(1.23)[-0.418,\ 0.447]}$	$\frac{p}{\delta_a}(s) = \frac{-3.53s(0.072)(0.106)e^{-0.0320s}}{(0.0987)(0.830)[-0.242,\ 0.461]}$
$\frac{r}{\delta_a}(s) = \frac{0.344(-0.345)[0.868,\ 0.487]e^{-0.00900s}}{(0.102)(1.23)[-0.418,\ 0.447]}$	$\frac{r}{\delta_a}(s) = \frac{0.353(0.658)[-0.0540,\ 0.240]e^{-0.0320s}}{(0.0987)(0.830)[-0.242,\ 0.461]}$
$\frac{a_z}{\delta_c}(s) = \frac{-0.00980s\ e^{-0.00740s}}{(0.105)}$	$\frac{a_z}{\delta_c}(s) = \frac{-0.00959s\ e^{-0.0320s}}{(0.122)}$
$\frac{q}{\delta_e}(s) = \frac{-2.66s(-0.271)(0.508)e^{-0.0656s}}{(0.105)(1.32)[-0.463,\ 0.579]}$	$\frac{q}{\delta_e}(s) = \frac{-2.30s(0.0280)(0.119)e^{-0.0320s}}{(0.122)(0.808)[-0.272,\ 0.499]}$

units: p, q, r : deg/sec
a_z : g
$\delta_a, \delta_e, \delta_r$: deg
δ_c : %

(2) It provides the Cramer-Rao-Bound, which is a measure of the reliability of each estimate.

(3) It yields the correlation between the identified parameters.

Both the Cramer-Rao-Bound and the parameter correlation help to develop an appropriate model structure and to avoid "over-parameterization." A nonlinear maximum likelihood method developed by DFVLR (Refs. 11, 12) was utilized for time-domain identification of the XV-15. This technique allows a general linear and nonlinear model formulation of the state and measurement equations:

$$\begin{aligned} x(t) &= f(x(t), u(t) - \Delta u, \beta) \qquad x(t = 0) = x_0 \\ y(t) &= g(x(t), u(t) - \Delta u, \beta) + \Delta y \end{aligned} \tag{8}$$

where

x = computed state vector
y = measured variables
u = measured control vector
x_0 = initial conditions
β = system parameters
$\Delta u, \Delta y$ = zero shifts

The initial conditions and zero shift terms are included to compensate for drifts and offsets in the measurements.

For the XV-15 data evaluation, the ML program was first utilized to check compatibility of the measurements, and to reconstruct the nonmeasured data. Then the program was used for the parameter identification itself. In the following sections, these steps are discussed in detail.

a. Data Compatibility and Reconstruction

The XV-15 instrumentation system provides attitude rates, attitude angles, and linear accelerations; speed measurements for the hover flight condition are not available. Therefore, only the compatibility of the angular data could be evaluated. A satisfactory agreement between calculated and measured angles was found and no additional corrections were made. For the frequency sweeps, speed components were derived by integrating the measured linear accelerations. Since, for these tests, the aircraft is in trim at the beginning and the end of each sweep, speed equation biases can be estimated to meet the boundary conditions: $u(0) = v(0) = w(0) = u(t_F) = v(t_F) = w(t_F) = 0$. For the system identification, the calculated velocity variables are included in the measurement vector together with the linear accelerations. Strictly speaking, these derived data do not provide additional information about the system dynamics; however, they help to keep the speed response of the model within a realistic range and to prevent long-term speed drifts. This characteristic is important since the identification procedures requires the integration of highly unstable (hover) system differential equations for a time duration of about 90 sec.

b. Identification of the Lateral/Directional Motion

Preliminary time-domain identification analyses showed that the longitudinal and lateral/directional motions of the XV-15 are practically decoupled. The main emphasis was placed on the identification of a linear lateral/directional model. This model is represented by (linear) differential equations for the lateral force, rolling moment, and yawing moments. The general 3 DOF model is:

$$\begin{aligned} \dot{x} &= Ax + Bu + bx \\ y &= Cx + Du + by \end{aligned} \tag{9}$$

where

$x^T = (v, p, r, \phi)$
$y^T = (a_y, v, p, r, \phi)$
$u^T = (\delta_a, \delta_r)$

The unknown coefficients in the state matrices (A and C) and the control matrices (B and D) are the desired stability and control derivatives. The bias vectors bx and by are estimated constants representing drifts and zero shifts.

In each flight test, a controller (either δ_a or δ_r) was used to excite the aircraft modes. To obtain sufficient information about both roll and yaw motion for the identification, data obtained from an aileron and a rudder sweep were combined. This "multiple run evaluation" yields one common model for both runs (except for the bias terms, which must be estimated for each individual run). This approach has been used successfully in previous helicopter identification studies (Ref. 5).

Three main characteristics of the XV-15 lateral/directional dynamics became obvious from the initial identification analysis:

The yaw motion which is due to rudder inputs is virtually decoupled and the significant parameters, yaw damping and the control derivative, can easily be extracted from the rudder-sweep data. Yaw-model and aircraft time histories are in good agreement.

There is some coupling from the aileron inputs to the yaw motion. Therefore, the control-coupling derivative N_{δ_a} was included for identification.

For the aileron-sweep data, it was not possible to obtain a satisfactory curve fit for the total run duration. The major difficulty is the identification of the roll-moment equation and, consequently, the fit of the roll-rate response.

The third characteristic caused some severe identification problems and was investigated in more detail.

One approach to this problem was to use shorter time intervals of the aileron sweep (only the low- or mid- or high-frequency part). With this approach, the responses of the identified models fit the measured roll rates almost perfectly. However, there were major differences in the estimated parameters from the original identification based on the total run duration. Tests with different a priori values to start the ML technique were also made to ensure that the ML criterion did not lead to local minima (a common identification problem). Results from these calculations clearly showed that the data contain strong nonlinearities which cannot be described by a linearized model. One logical next step is the extension of the model to include the appropriate nonlinearities; this extension will be addressed later. Another possibility is to stay with a linear model, accept its deficiencies, and define its range of validity and applicability. This approach is discussed first.

Lateral/directional model identification was conducted separately on the three available aileron-sweep runs, each in combination with a rudder-sweep run. When the total run duration was used, all three sweep results showed the same tendency:

The model response matched the low-frequency part of the data fairly well.

The model response underestimated the flight data as the input frequency increased, with up to a 50% error in roll rate at high-input frequencies.

These results make sense in light of the ML identification criterion:

$$L = \sum_{i=1}^{N} [(z(t_i) - y(t_i))^T \cdot R^{-1} \cdot (z(t_i) - y(t_i))] + N/2 \cdot \ln |R| \tag{10}$$

where

N = number of data points
z = measurement vector
y = model response vector
R = measurement noise covariance matrix

The optimum is reached when the differences between the amplitudes of the measured and calculated time histories are minimized. From Fig. 4b, it is seen that about 70% of the total run duration of the aileron-sweep is low-frequency data. Consequently, the identification method emphasizes primarily the longer-duration, low-frequency part of the data, and sacrifices the accuracy of the shorter, high-frequency part. For many applications, the initial and short term (higher-frequency) response of a system is of more interest than the long term (lower-frequency) behavior. Therefore, it was desirable to improve the identification result for the higher-frequency range, allowing larger errors for the low frequencies. Methods to meet this objective are:

i. Conduct frequency-sweeps with more emphasis on the high-frequency content.

ii. Apply alternate control inputs (e.g., multisteps) which excite mostly the mid- and high-frequency dynamics.

iii. Use only the higher-frequency sweep data for the identification.

These approaches were either not possible (new flight testing required for options i and ii) or they were felt to be a poor compromise (iii).

Another solution is to increase the influence of the amplitude errors for a selected part of the data. When frequency-sweep inputs are used, this can be done by the "multiple segment evaluation": a part of the data (e.g., high-frequency range) is treated as a separate test. It is combined several times with the original test data so that, in principal, the weighting of the chosen data points is arbitrarily increased. This approach worked satisfactorily, but it yielded an increased number of unknown biases, needed more data handling and, in particular, required more computing time. But pursuing this basic idea, the identification program was modified to allow different weighting of selected time periods within one run. This approach turned out to be very efficient as it does not require estimating any additional parameters, or computing capacity.

The data weighting technique was applied for the identification of the aileron frequency-sweeps. Increased weights were used for the roll-rate fit errors which occurred in the higher-frequency part of the data. Good agreement of the measured and calculated data was thus obtained for the mid- and high-frequency inputs, whereas there were larger discrepancies for the low-frequency inputs. Also, there was good consistency of results for the three repeat runs. The results also confirmed that it is advantageous to keep the low-frequency data in the evaluation as they provide the necessary speed-derivative information. The mean values and standard deviations for the derivatives obtained from the identification of the aileron sweeps are summarized in Table 2. As time-domain techniques tend to be sensitive to phase shifts, a time lag for the control input was estimated as a multiple of the sampling rate. In state-space format, the final time-domain identification (mean-value) model for the lateral/directional motion is:

$$\begin{bmatrix} \dot{v} \\ \dot{p} \\ \dot{\phi} \\ \dot{r} \end{bmatrix} = \begin{bmatrix} -0.0749 & 0 & 9.81 & 0 \\ -0.0179 & -0.559 & 0 & -0.349 \\ 0 & 1 & 0 & 0 \\ 0.00140 & 0 & 0 & -0.0715 \end{bmatrix} \begin{bmatrix} v \\ p \\ \phi \\ r \end{bmatrix} + \begin{bmatrix} -0.0112 & 0 \\ -0.0617 & 0 \\ 0 & 0 \\ 0.00615 & 0.0128 \end{bmatrix} \begin{bmatrix} \delta_a \\ \hline \delta_r \end{bmatrix}^{*} \tag{11}$$

units: v : m/sec
p, r : rad/sec
ϕ : rad
δ_a, δ_r : deg

*Time delay in control input is $\tau = 0.0320$ sec.

Figure 8 gives the time-history comparison for one of the sweeps with the state-space model. Once again, this final time-domain model correlates well at medium and high frequency, with some discrepancy at low frequency. Overall, however, the agreement is quite satisfactory.

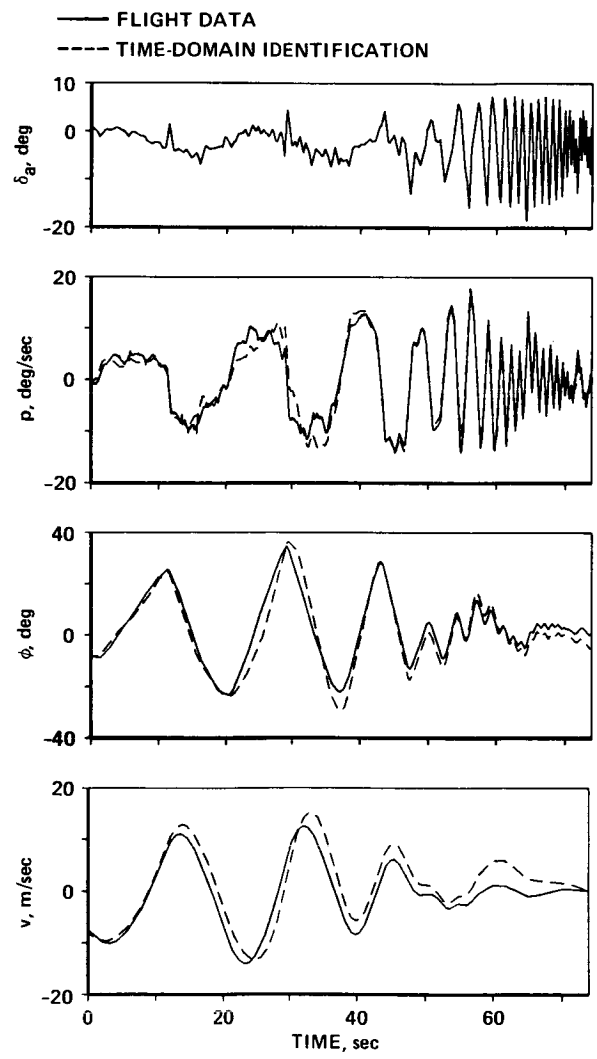

Fig. 8. Time-domain identification of lateral/directional model.

The present XV-15 study is the first experience with explicit data weighting. This technique certainly requires further development and, as with all such weighting methods, should be used very carefully. In this regard, the comparison with the frequency-domain results is very helpful in evaluating the confidence and the range of validity of the results.

c. Identification of the Longitudinal Motion

For the identification of the longitudinal model, an elevator sweep test was combined with a power sweep test. The identification results for the longitudinal dynamics were analogous to the preceding lateral/directional results:

The heave equation is practically decoupled and can easily be identified from the power sweep tests to obtain the vertical damping and the control derivatives.

The elevator sweep showed the same tendency as the aileron sweeps: it was not possible to determine a model that is equally good for the low- and high-frequency range. Again, the main problem occurred in the moment equation so that the discrepancies were seen in the pitch-rate comparison.

Only one of the three available flight tests could be evaluated. When the other two tests were used, the identification results diverged and became unusable. This is in agreement with the frequency-domain analysis which also indicated some problems with these runs. For the one remaining elevator sweep run, the first 30 sec of data had to be removed in order to reach convergence in the estimation. Again, the data-weighting technique was successfully used to obtain a satisfactory fit for the higher frequency part of the data. The longitudinal model parameters are given in Table 2. Unfortunately, the identified longitudinal model is based on only a rather limited amount of data. Therefore, except for the heave equation, this model cannot be expected to have the same level of reliability as the lateral/directional model. However, the good comparison with the frequency-domain results as discussed in the next sections show that the time-domain model accurately represents the XV-15 longitudinal dynamics.

TABLE 2 Time-Domain Identification Results

Derivative	Mean	Variance	Standard Deviation	Standard Deviation (% of mean value)
a) Lateral/Directional Parameters (3 runs)				
Y_v	-0.0749	2.04×10^{-4}	0.0143	-19.1
L_v	-0.0179	5.67×10^{-6}	0.00238	-13.3
Y_{δ_a}	-0.0116	1.41×10^{-7}	0.000376	-3.37
L_p	-0.559	1.03×10^{-2}	0.101	-18.1
N_v	0.00141	3.45×10^{-6}	0.00186	132.
L_r	-0.349	1.33×10^{-2}	0.115	-33.0
L_{δ_a}	-0.0617	3.00×10^{-6}	0.00173	-2.81
N_{δ_a}	0.00615	2.15×10^{-7}	0.000463	7.53
N_r	-0.0715	6.00×10^{-6}	0.00245	-3.42
N_{δ_r}	0.0127	1.78×10^{-7}	0.000422	3.30
b) Longitudinal Parameters (1 run)				
X_u	-0.0636			
X_w	0.0175			
X_{δ_e}	0.0939			
Z_u	-0.0685			
Z_w	-0.122			
Z_{δ_e}	-0.0469			
Z_{δ_c}	-0.00959			
M_u	0.0204			
M_w	-0.00160			
M_q	-0.477			
M_{δ_e}	-0.0401			

units: u,v,w : m/sec
p,q,r : rad/sec
$\delta_a,\delta_e,\delta_r$: deg
δ_c : %
X,Y,Z : n
L,M,N : n-m

4. COMPARISON OF IDENTIFICATION RESULTS

This section compares the frequency- and time-domain identification results. This comparison is done in frequency- and time-domain formats, since both are important for ensuring model fidelity. In the frequency-domain format, transfer-function parameters from the frequency-domain identification are compared with those obtained from the state-space formulation. Also, frequency responses from the two models are compared with the flight-data frequency response. Since the frequency-domain format is the "natural environment" for frequency-domain identification, the models obtained from this approach generally fit the flight-data responses better than those obtained from time-domain identification. Comparison in the time-domain format is achieved by driving the frequency-domain models with the frequency-sweep input histories. The resulting responses are compared with the responses of the vehicle and the time-domain identification fits. Since this is the "natural environment" for time-domain identification, models identified using this approach generally match the flight data better here. (The detailed discussion of the results for the roll-axis is continued, and the results for the remaining axes are again summarized.)

A. Comparison in the Frequency-Domain Format

Transfer functions are obtained from the time-domain identification results of Eqn. 11 (and Table 2) by Cramer's rule, and are tabulated for comparison with the frequency-domain results in Table 1.

(1) Lateral/directional Models

The results of Table 1 indicate that the lateral/directional modes (denominator factors of the transfer functions) are nearly identical for both techniques, except for the difference in the unstable damping ratio (ζ_R). The high-frequency gain and time delay of the three transfer-functions compare very well, while there are some differences in the low-frequency numerator factors.

The relative significance of the differences in the transfer-function parameters can be more clearly seen from the frequency-response comparison of the models with the flight data. The roll responses of the identified models and the aircraft are shown in Fig. 9. At frequencies of $\omega > 1$ rad/sec, both models correspond almost exactly with the flight data. Also, both models correctly predict a low-frequency instability at $\omega = 0.5$ rad/sec, with a falling magnitude response for lower frequencies.

A closer examination of the magnitude and phase comparisons shows that the frequency-domain identification result matches the magnitude-response curve better than the time-domain identification result in the vicinity of the dominant mode ($\omega = 0.5$ rad/sec). However, the time-domain identification result matches the phase-response curve better in this frequency-range. This difference is due entirely to the inherent weighting of the two methods. In the frequency-domain identification method, the relative weighting between magnitude and phase is arbitrary, but the standard choice (1 DB error: 7° error) has produced satisfactory results in a number of identification studies conducted by one of the authors (Refs. 1-4). In time-domain identification, the performance index is much more sensitive to phase errors, which generate a large area between the model and flight-data responses. Thus, the phase response is more closely matched. Also, time-domain identification results can be highly sensitive to the identified value of time-delay, which must be an integral multiple of the sample rate.

The fact that magnitude and phase curves cannot be matched simultaneously in either frequency or time-domain identification methods further indicates the existence of important nonlinearities in the low-frequency roll oscillation modes. Therefore, linear models (from either method) are a compromise and cannot fully characterize the nonlinear behavior of the vehicle. Both methods capture the important vehicle response characteristics and are generally in good agreement with each other. Similar agreement is also exhibited in the yaw responses to rudder (r/δ_r) and aileron (r/δ_a) inputs.

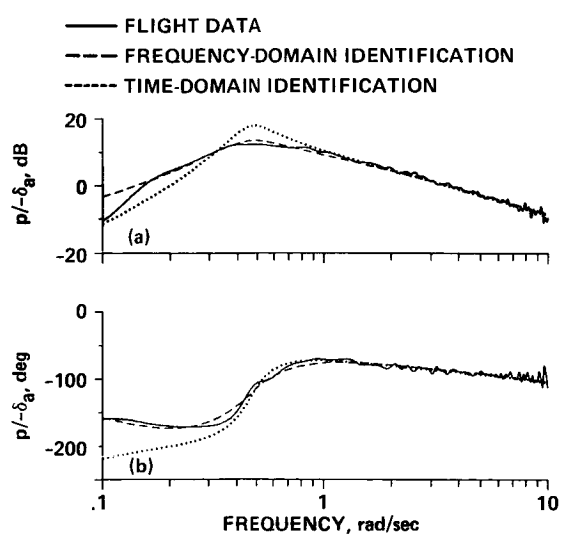

Fig. 9. Comparison of roll-response models ($p/-\delta_a$) in the frequency-domain format. a) Magnitude; b) phase.

(2) Longitudinal Models

The comparison of transfer-function models for the longitudinal degrees-of-freedom is very similar to the preceding results for the lateral/directional degrees-of-freedom. The dominant modes of motion for the two methods are very close, except for the difference in the unstable damping ratio, ζ_p (again roughly a factor of 2). The high-frequency gain and time delays of the two transfer functions are also nearly identical, with some differences in the low-frequency numerator parameters. As before, the frequency-response match between the two models and the flight data is nearly identical for frequencies greater than 1 rad/sec. Also, in the frequency range near the dominant mode (ω = 0.5 rad/sec), the frequency-domain model fits the magnitude response better, while the time-domain model fits the phase response better. Once again, nonlinearities and differences in inherent weighting of the methods is the cause of this discrepancy. In general, however, the agreement between the models and the flight data is quite satisfactory.

B. Comparison in the Time-Domain Format

Transfer functions obtained from the frequency-domain identification were converted into a canonical state-space representation to generate time histories for the comparison with the flight-test data. A bias term was estimated for each equation (using a least-squares procedure) to compensate for zero shifts and drifts. Figure 10 shows an aileron-sweep time history compared with the frequency-domain identified model, and the time-domain identified model. For the high-frequency inputs, both models yield virtually the same result and agree with the flight-test data. In the lower frequency range, some differences between the two models and differences with the flight-test data can be seen. Generally, the agreement with the flight data is quite satisfactory, so it can be stated that both identified models represent the dynamics of the aircraft fairly well. The discrepancies between the two model responses, however, indicate that no unique model can be identified; the slightly different results reflect the specific identification criterion of each method. This confirms the preceding conclusions from the comparison in the frequency-domain format.

5. TIME-DOMAIN VERIFICATION USING STEP-RESPONSE DATA

A good way to judge the utility of the identification results is to compare the prediction of the identified models with the vehicle response for inputs other than those which were used in the identification procedure. Here, step inputs are used since these are quite different from the frequency-sweep forms which are used in identification. (These step inputs tended to be very rounded in nature, so low-pass, preconditioning to remove high-frequency elements of the input signal is not necessary as was done in Ref. 4.)

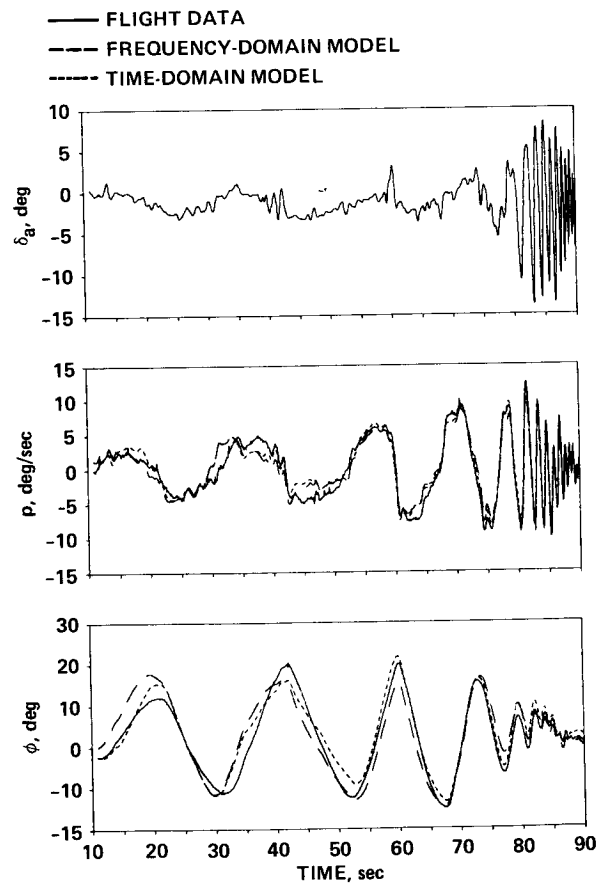

Fig. 10. Comparison of roll-response models in the time-domain format.

A. Lateral/Directional Motion

The identification of the yaw motion did not cause any difficulties. Therefore, a satisfactory prediction capability can be expected. Figure 11 compares the yaw-rate model responses with the measured data for a pedal-step input. Good agreement is apparent for both models. The small discrepancies are caused by an inaccurate calibration factor between pedal and rudder (surface) deflection, and some mid-frequency mismatch of the first-order yaw model (Ref. 9).

Identification problems associated with the aileron-sweep evaluation have been discussed in detail. The verification using step input data offers a good possibility to check the validity of the linear models. Lateral stick step-inputs were flown with the roll SCAS-off and the yaw SCAS-on; so the measured yaw-rate response shown in Fig. 12 results from the pilot's lateral stick and pedal inputs, and the yaw-SCAS activity. The comparison of the roll rate (p) and roll angle (ϕ) response proves that both models are able to predict accurately the aircraft motion. This agreement is also true for the yaw rate comparison which indicates that the coupling derivative (N_{δ_a}) was correctly identified. Minor differences between the two model responses probably result as before from the different weighting methods.

B. Longitudinal Motion

The heave response is practically decoupled and gave no problems in either identification method; good verification results are expected. Figure 13 shows that the power step responses agree with the measured (quite noisy) vertical acceleration data. The responses are shown separately for the two models since they are practically identical and cannot be distinguished when shown within the same plot.

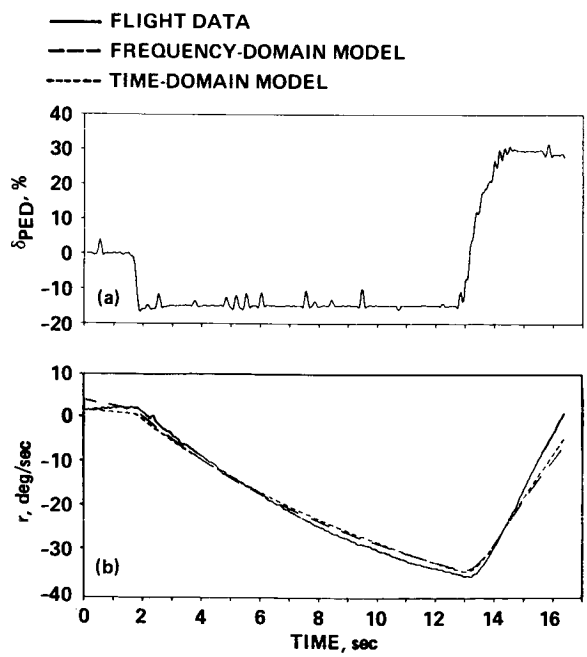

Fig. 11. Comparison of yaw-rate response prediction for step rudder input (yaw SCAS-off). a) Pedal input ±100% δ_{ped} = ±44 deg δ_r; b) yaw-rate response.

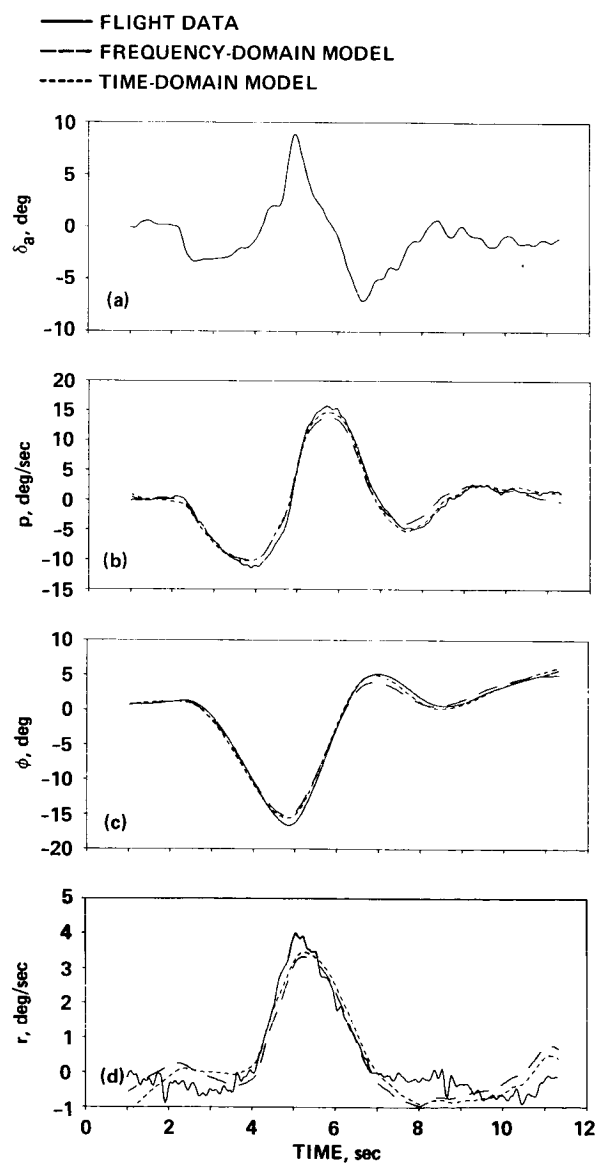

Fig. 12. Comparison of lateral/directional response prediction for step aileron input (roll SCAS-off, yaw SCAS-on). a) Aileron input; b) roll rate; c) roll angle; d) yaw rate.

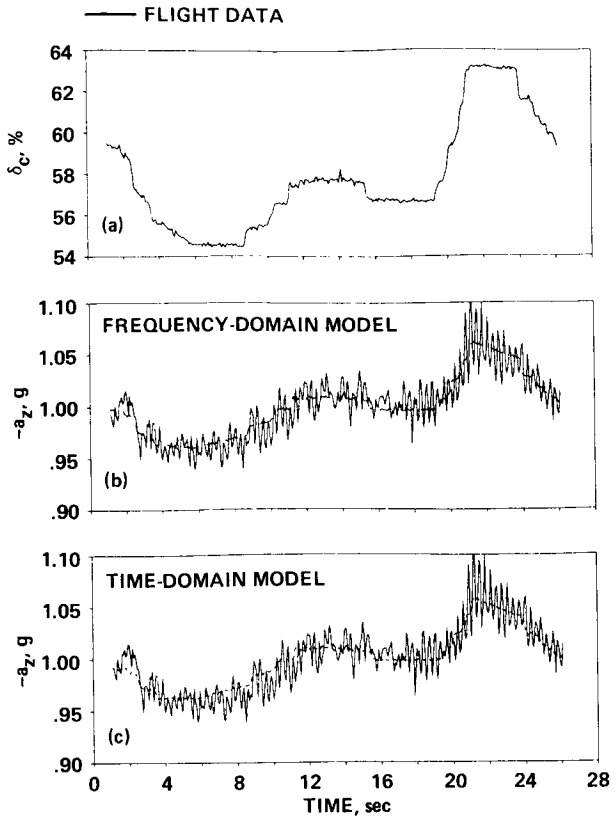

Fig. 13. Comparison of vertical-acceleration response prediction for step power lever input. a) Power lever input; b) frequency-domain model; c) time-domain model.

Nonlinearities and a limited pitch-response data base led to problems in identifying a longitudinal model, as has been discussed. Therefore, the verification tests using elevator steps are particularly helpful in checking the reliability of the two models. Figures 14 and 15 compare the pitch-model responses for two different flight conditions: pitch SCAS-off and pitch SCAS-on. In both cases, the identified models yield a good prediction of the aircraft response. Again, the minor differences between the responses are due to the inherent weighting of each method.

The SCAS-off data fit of Fig. 14 is of special interest. Since the models were extracted from SCAS-on flight-test data, some output/input correlation cannot be avoided and may lead to significant identification errors; in the worst case, the inverse feedback transfer function rather than the open-loop aircraft response would be identified (Ref. 9). However, the good agreement between the model time histories and the SCAS-off flight data in Fig. 14 clearly demonstrates that the open-loop dynamics of the aircraft were determined. The overall excellent correlation of the models and step-response data adds confidence to the accuracy of identified derivatives and transfer functions, and the estimation techniques.

6. NONLINEAR MODEL IDENTIFICATION

The preceding identification results from both time- and frequency-domain techniques have demonstrated that linear model identification yielded a compromise between low- and high-frequency data fits, or between magnitude- and phase-response fits. They suggest the existence of significant nonlinearities, particularly in the roll and pitch axes. Therefore, the nonlinear maximum likelihood time-domain method was utilized to identify an extended model and to investigate the importance of various parametric terms.

Relatively large amplitude aircraft responses during the low-frequency inputs (see, for example, Fig. 8) are a common characteristic of all of the frequency-sweep flight-test data. Deviations from the steady-state trim are in the range of:

9-14 m/sec in lateral speed (aileron-sweep)

8-11 m/sec in longitudinal speed (elevator-sweep)

25-37 deg in roll angle (aileron-sweep)

17 deg in pitch angle (elevator-sweep)

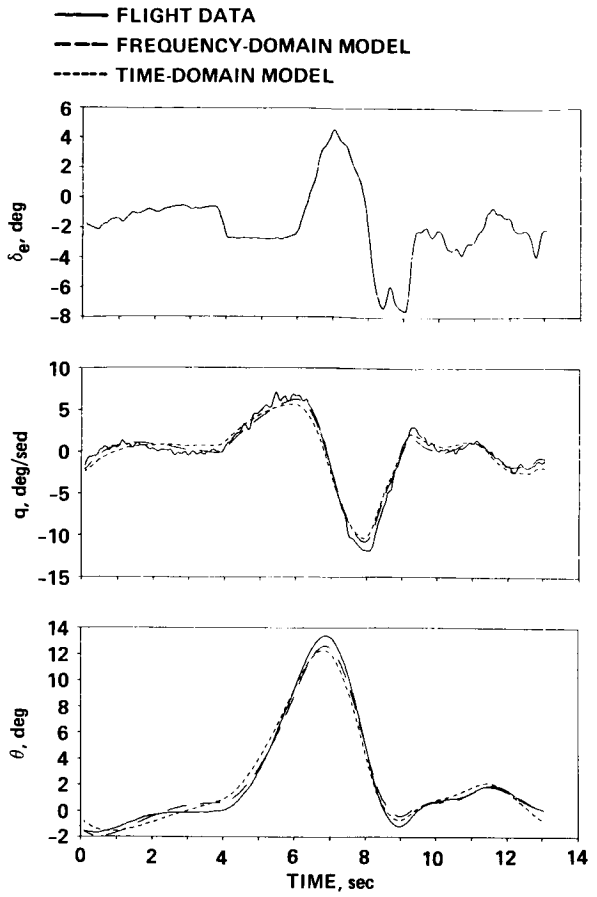

Fig. 14. Comparison of pitch-response prediction for step elevator input (pitch SCAS-off).
a) Elevator input; b) pitch rate; c) pitch angle.

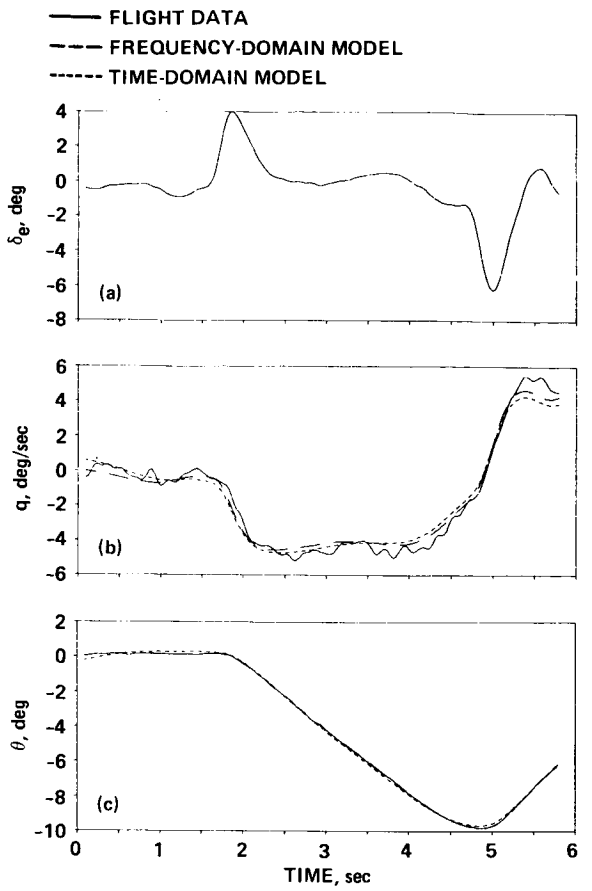

Fig. 15. Comparison of pitch-response prediction for step elevator input (pitch SCAS-on).
a) Elevator input; b) pitch rate; c) pitch angle.

These amplitudes are certainly large enough to violate the small-perturbation assumptions for linear models; further, the dynamic characteristics of hovering rotorcraft are especially sensitive to translational speed changes. Therefore, the linear model was first extended by adding nonlinear speed derivatives (L(v**2) and L(v**3)) to the roll moment equation: the curve-fits improved significantly, in particular owing to L(v**2). Further attempts to reduce the remaining discrepancies were made by including additional nonlinear terms. Their significance was checked with time-history comparisons and the evaluation of the parameter covariance matrix, which indicates the reliability of the identified parameter and the correlation with other parameters. As a preliminary result, a model was identified that includes the above mentioned speed derivatives and, in addition, L(δ_a**2) and L(δ_a*u).

Figure 16 shows that the nonlinear model fits the measured data almost perfectly. The results presented in Fig. 16 are preliminary and are intended to illustrate the possible role of nonlinearities in the dynamics. It is important to note that the model was identified without the use of any explicit data weighting. This suggests that the additional weighting (e.g., high frequency versus low frequency) is not required when an appropriate model formulation is applied. However, the evaluation again revealed a well known identification problem: it is always possible to improve the time-history curve fit by arbitrarily adding model parameters. But, a useful model requires the estimated derivatives to have physical significance. It is the responsibility of the analyst to define and select meaningful additional terms. For the side-by-side rotor configuration of the XV-15, the speed-related derivatives (L(v**2) and L(v**3)) are physically justified. Similarly, the control effectiveness may be in fact nonlinear and dependent on forward speed; but these effects should be further investigated.

7. ASSESSMENT OF IDENTIFICATION METHODS

This cooperative study has provided the unique opportunity for specialists using different methods to compare and coordinate analyses of a common rotorcraft data base. This experience has been invaluable for gaining a better appreciation for the advantages and limitations of both techniques, and for formulating ideas for an integrated approach to dynamics identification. The following observations are based on the results of this cooperative effort.

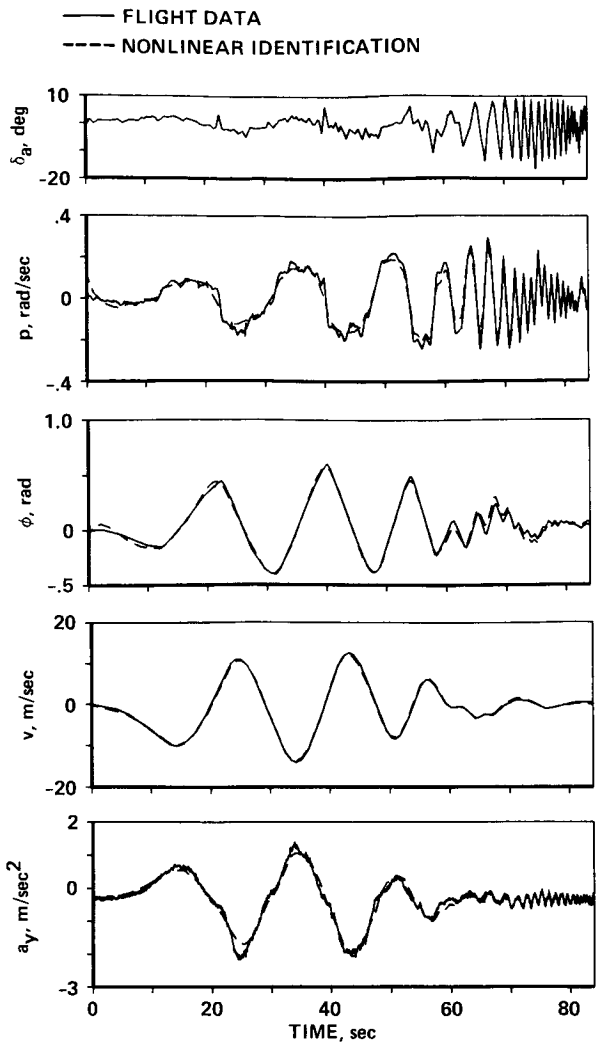

Fig. 16. Example of time-domain identification of a nonlinear lateral/directional model.

The principal advantages of frequency-domain identification are:

a. Frequency responses of the dominant on-axis input/output pairs are rapidly generated and are very useful for gaining a good appreciation for the inherent vehicle dynamics. The fact that the extracted frequency-responses are independent of pre-assumed models is important for the initial assessment of natural system order, dominant-mode locations, and stability characteristics. As a result, a better choice of appropriate model structure and order is possible.

b. Parameters associated with the high-frequency dynamic behavior can be determined directly from the frequency-responses without any a priori assumption of model structure. Specifically, the control derivatives (e.g., $L_{\delta_a}, M_{\delta_e}$) are determined from the high-frequency gain responses, and the equivalent time delays (e.g., τ_ϕ, τ_e) are determined from the high-frequency phase responses.

c. Weighting can be accomplished explicitly. Relative weights can be arbitrarily assigned to the magnitude and phase curves. Model fitting can also be arbitrarily weighted more to the low- or high-frequency range--depending on the intended use of the model.

d. Accurate, high-resolution frequency-response identification is given the main emphasis in this method. CHIRP z-transform methods are especially well suited for identifying frequency-responses from noisy flight data. The resulting transfer-function models are a much closer representation of the frequency-response characteristics than is possible with time-domain identification.

The principal disadvantages of frequency-domain identification are:

a. Current techniques are not well suited for highly coupled multi-input/multi-output (MIMO) system identification, although two-input/single-output identification has been successfully attained in the present study. More highly automated techniques are needed to make the frequency-domain methodology efficient when the required number of input/output frequency-responses is large. Also, methods for simultaneous fitting of many coupled responses is necessary to ensure commonality of transfer-function denominator parameters for MIMO models.

b. Frequency-domain identification results in transfer-function models. Individual stability derivatives are not readily extracted unless the assumed models are of very low order.

c. Spectral analysis assumes input-to-output linearity. For nonlinear systems, the transfer functions are linearized describing functions; identification of pure nonlinear parameters is not possible.

The principal advantages of time-domain identification are:

a. The method is naturally suited to multi-input/multi-output identification since the model can be of arbitrary order and structure. This method is especially well suited for identifying highly coupled systems.

b. Stability and control derivatives are identified explicitly, and the method leads to the identification of a complete state-space model.

c. Considerable effort is invested in achieving the highest quality of time-domain data. Data consistency, drop-out tests and signal-reconstruction methods are an integral part of the time-domain identification procedure. The least-squares fitting in the time-domain with high-quality time-history data results in a much better time-domain fit of the frequency-sweep responses.

d. Extended maximum-likelihood techniques can be used to identify parametric nonlinearities which are especially important in the low-frequency dynamics of hovering rotorcraft.

The principal disadvantages of time-domain identification are:

a. The results are dependent on presumed model structure and order. When a new configuration is being identified, a priori knowledge of model structure may not be available, and considerable variation in the parameters can occur when the model structure is altered.

b. Explicit frequency-domain weighting is not possible. Specifically, the time-domain method inherently weights phase errors more heavily than magnitude errors. This characteristic makes the extracted state-space model very sensitive to pure time delays and unmodeled high-frequency dynamics. Also, the method inherently weights low-frequency dynamics much greater than high-frequency dynamics; this weighting can be adjusted when the input signal has monotonically increasing frequency content as in the frequency-sweep.

c. Confidence in the individual state-space model parameters may be very low since the identified state-space model can contain a high degree of internal cancellation in the overall input-to-output response.

8. A PROPOSAL FOR A COORDINATED FREQUENCY-DOMAIN/TIME-DOMAIN IDENTIFICATION METHOD

The preceding assessment of the advantages and limitations of each identification method suggests the following coordinated frequency-domain/time-domain identification approach:

Step 1. Use time-domain signal conditioning methods to clean up the flight data for drop-outs, wild points, and consistency. For example, rate gyros can be integrated and compared with attitude gyros.

Step 2. Identify the dominant input/output on-axis frequency-response characteristics using only the best runs, as determined from coherence analyses of the individual frequency-sweeps. Identify the effective time delay and high-frequency control sensitivity directly from the frequency-response plots.

Step 3. Formulate low-order system models from inspection of the identified frequency-response plots and theoretical analyses. Determine the on-axis transfer-function parameters.

Step 4. Formulate a state-space model which has a structure and order consistent with the transfer-function model formulation. Time-domain identification should be completed with the equivalent time delay fixed at the value identified in Step 3. Weighting should be applied to the time-history data to ensure that the control sensitivity derivatives are maintained at the value identified in Step 3. (Alternatively, the control derivatives can be fixed.)

Step 5. Compare the extracted on-axis transfer-functions, frequency-responses and time histories from the time-domain and frequency-domain results. If substantial errors exist, go back to Step 2; reevaluate the quality of the spectral-responses, time responses, and the order and structure of the selected models. If the models are found to be the best which can be achieved under the assumption of linearity, pursue nonlinear maximum-likelihood methods to identify the dominant parametric nonlinearities.

Step 6. Verify the extracted models using time-history data from inputs not used in the identification procedure. If significant errors between the predicted and actual response characteristics exist, reevaluate the significance of observed discrepancies in frequency and time-domain identification fits. If necessary, go to Step 3 and increase the order of the models; but, check for the possibility of model over-parameterization by trying a few different verification inputs.

9. CONCLUSIONS

This joint effort has provided the unique opportunity for specialists in different techniques to compare their approaches using a common flight test data base. On the basis of this comparison, it has been shown that the frequency and time-domain methods each have important advantages and inherent limitations. Future identification efforts must be based on a comprehensive, coordinated approach which uses both frequency and time-domain methods.

REFERENCES

1. Tischler, M. B., Leung, J. G. M., and Dugan, D. C., "Frequency-Domain Identification of XV-15 Tilt-Rotor Aircraft Dynamics in Hovering Flight," AIAA Paper 83-2695, AIAA/AHS 2nd Flight Testing Conference, Las Vegas, November 1983. (Also published in condensed version in J. Amer. Helicopter Soc., Vol. 30, No. 2, April 1985, pp. 38-48.)

2. Tischler, M. B., Leung, J. G. M., and Dugan, D. C., "Identification and Verification of Frequency-Domain Models for XV-15 Tilt-Rotor Aircraft Dynamics in Cruising Flight," AIAA Journal of Guidance, Control, and Dynamics, July-August 1984, Vol. 9, No. 4, pp. 446-453.

3. Tischler, M. B., Fletcher, J. W., Diekmann, V., Williams, R. A., and Cason, R., "Demonstration of Frequency-Sweep Flight Test Technique Using a Bell 214-ST Helicopter," work in preparation (1986).

4. Chen, R. T. N., and Tischler, M. B., "The Role of Modeling and Flight Testing in Rotorcraft Parameter Identification," 1986 AHS Forum, System Identification Session, 2-4 June 1986, Washington, DC.

5. Kaletka, J., "Rotorcraft Identification Experience," AGARD-LS-104, Nov. 1979, pp. 7-1 to 7-32.

6. Kaletka, J., "Practical Aspects of Helicopter Parameter Identification," AIAA CP849, 1984, pp. 112-122, AIAA No. 84-2081.

7. Hoh, R. H., Mitchell, D. G., Ashkenas, I. L., Aponso, B. L., Ferguson, S. W., Rosenthal, T. J., Key, D. L., and Blanken, C. L., "Proposed Airworthiness Design Standard: Handling Qualities Requirements for Military Rotorcraft," System Technology, Inc. TR-1194-2, 20 Dec. 1985.

8. Kaletka, J., Langer, J.-J., "Correlation Aspects of Analytical, Wind Tunnel and Flight Test Results for a Hingeless Rotor Helicopter," AGARD-CP-339, 1982, pp. 16-1 to 16-16.

9. Tischler, M. B., "Frequency-domain Identification of XV-15 Tilt-Rotor Aircraft Dynamics," Ph.D. Dissertation, Stanford University, Stanford, California, work in preparation (1986).

10. Hoh, Roger H., Mitchell, David G., Ashkenas, Irving L., Klein, Richard H., Heffley, Robert K., and Hodgkinson, J., "Proposed MIL Standard and Handbook--Flying Qualities of Air Vehicles, Vol. II: Proposed MIL Handbook," AFWAL-TR-82-3081, 1982.

11. Jategaonkar, R., and Plaetschke, E., "Maximum Likelihood Parameter Estimation from Flight Test Data for General Nonlinear Systems," DFVLR-FB 83-14, 1983.

12. Jategaonkar, R., and Plaetschke, E., "Nonlinear Parameter Estimation from Flight Test Data Using Minimum Search Methods," DFVLR-FB 83-15, 1983.